

Optically Induced Hybridization of a Quantum Dot State with a Filled Continuum

P. A. Dalgarno,¹ M. Ediger,¹ B. D. Gerardot,¹ J. M. Smith,¹ S. Seidl,² M. Kroner,² K. Karrai,² P. M. Petroff,³
A. O. Govorov,⁴ and R. J. Warburton¹

¹*School of Engineering and Physical Sciences, Heriot-Watt University, Edinburgh EH14 4AS, United Kingdom*

²*Center for NanoScience and Department für Physik, Ludwig-Maximilians-Universität, 80539 München, Germany*

³*Materials Department, University of California, Santa Barbara, California 93106, USA*

⁴*Department of Physics and Astronomy, Ohio University, Athens, Ohio, USA*

(Received 31 May 2007; revised manuscript received 14 January 2008; published 28 April 2008)

We present an optical signature of a hybridization between a localized quantum dot state and a filled continuum. Radiative recombination of the negatively charged trion in a single quantum dot leaves behind a single electron. We show that in two regions of vertical electric field, the electron hybridizes with a continuum through a tunneling interaction. The hybridization manifests itself through an unusual voltage dependence of the emission energy and a non-Lorentzian line shape, features which we reproduce with a theory based on the Anderson Hamiltonian.

DOI: [10.1103/PhysRevLett.100.176801](https://doi.org/10.1103/PhysRevLett.100.176801)

PACS numbers: 73.21.La, 78.67.Hc

The hybridization between a localized quantum state and delocalized continuum states is a recurring and powerful theme in quantum physics. A famous example in transport is the Kondo effect, the process whereby a single electron spin is screened through a coherent coupling to an electron gas. This effect was originally discovered in metals doped with magnetic atoms but has enjoyed a resurgence of interest recently as Kondo physics is prominent when a spin-half nanosystem, for instance a single molecule [1], carbon nanotube [2], or quantum dot [3], is coupled to metallic leads. In the context of optics, quantum interferences occur when a localized initial state has an optical dipole transition both to a high energy localized state and to a degenerate continuum. When an electron in the high energy localized state has an interaction with the continuum, the linear optical response has characteristically asymmetric line shapes, Fano resonances [4]. However, the optical response when the continuum is occupied with electrons and brought into the Kondo regime is much less well understood.

Self-assembled quantum dots are ideally suited to probing these hybridizations. The dots themselves have highly confined states with a strong optical dipole transition across the fundamental energy gap. Significantly, the dots can be incorporated into semiconductor heterostructures allowing the continuum states to be engineered. Despite this, the prevailing view in this field is that the continuum states are only problematic, a source of dephasing. We take the opposite view here. We establish a strong tunneling interaction between a quantum dot and an occupied continuum by applying a vertical electric field. In two windows of electric field, we find that detection of photon emission from a trion in a single dot projects the remaining electron into a hybridization of quantum dot and continuum states. The signatures are an unusual dependence of the energy on electric field and non-Lorentzian line shapes. Our results agree well with a theory based on the Anderson Hamiltonian and a frozen Fermi sea. In one of these

voltage ranges, the final state electron tunnels out of the dot. The coherent part of the process is that the electron has a chance to tunnel back into the dot, and this leads to the unusual dispersion and line shapes.

The quantum dots are self-assembled by MBE and consist of highly alloyed InGaAs. The dots are highly inhomogeneous, emitting from 920 to 980 nm, allowing us to explore a large range of parameters by moving from one dot to the next. The dots are separated by 25 nm from a Fermi sea, a grounded 20 nm thick n^+ GaAs layer (doping $\sim 10^{18} \text{ cm}^{-3}$). A voltage is applied to a Schottky barrier on the sample surface, 150 nm above the dots, generating a vertical electric field. An AlAs/GaAs superlattice between the dots and the surface inhibits a photocurrent on non-resonant optical excitation with a laser diode at 850 nm (dot *A*) or 826 nm (dot *B*). We measure the photoluminescence (PL) of individual quantum dots as a function of gate voltage, V_g , with a spectrometer-detector system with resolution 50 μeV . There is a clear Coulomb blockade, Fig. 1: as the bias increases, the charge of the lowest configuration changes abruptly, starting with the dark hole-only state, h , with a transition to the neutral exciton X^0 , and then to the negatively charged trion X^{1-} [5]. Nonresonant optical excitation provides the minority carrier, the hole, the electron Fermi sea the majority carriers, the electrons. Following hole capture, electrons tunnel in or out of the dot in order to minimize the energy. For our structure, we have determined the tunneling time to be typically 10 ps for dots at the red end of the ensemble spectrum, decreasing to 2 ps at the blue end of the spectrum. We do this by measuring the dark to bright exciton spin flip time which is limited in these structures by a spin-swap process with the back contact, a process which depends sensitively on the electron tunneling time [6]. The focus here is on the ~ 10 dots we have investigated with particularly short tunneling times, ~ 0.5 ps.

We have discovered striking and anomalous behavior at the X^0 - X^{1-} transition. Two examples are shown in Fig. 1

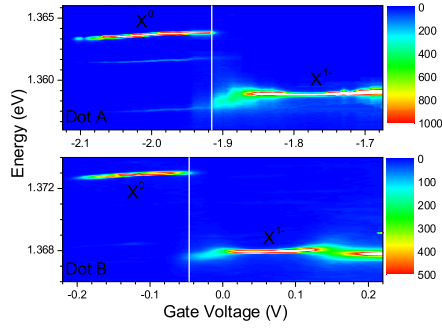


FIG. 1 (color online). Measured PL intensity versus gate voltage V_g from two single InAs/GaAs quantum dots (A and B) at nominally 4 K. The scale bar relates to detector counts. The solid lines mark the X^0 to X^{1-} transitions.

(dots A and B). Right up to the high- V_g end of the X^0 plateau, the X^0 PL is intense and spectrally narrow. The small V_g -dependence of the X^0 PL energy arises from the Stark effect. However, at the low- V_g end of the X^{1-} plateau, the X^{1-} PL is broad. Increases of V_g cause the X^{1-} PL first to blueshift, then to redshift, with an accompanied rapid line narrowing. These shifts are much larger than those expected from the Stark effect. Figure 2 shows the line shapes for dot A. Significantly, at the point of maximum blueshift, the X^{1-} PL line shape is non-Lorentzian, with a low energy tail. These effects are features of all the dots studied and are particularly strong for the dots on the blue end of the ensemble spectrum.

Within the X^{1-} plateau, once a hole has been generated by the optical excitation, the ground state configuration contains 2 electrons and has an energy below the Fermi energy of the Fermi sea. The anomalous behavior in Fig. 1 is therefore unlikely to be related to the initial state of the PL process; we show instead that it arises from interactions in the final state. After detection of X^{1-} recombination, a

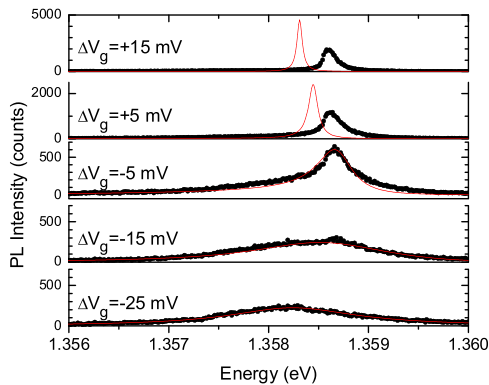


FIG. 2 (color online). X^{1-} PL measured from dot A and calculated with the theoretical model (solid lines). The theory uses $\Delta = 1.35$ meV, $\gamma = 5$ μ eV, $T = 6$ K, $E_1 = 30$ meV, $E_2 = 30$ meV, $E_{ee} = 22.2$ meV, $I_0 = 492$ counts with an unperturbed X^{1-} PL at 1.357580 eV and $|e\rangle - |2e\rangle$ crossover at -1.875 V. The calculated curves are convoluted with a Lorentzian with full width 50 μ eV in order to take account of the response of the detector system in the experiment.

single electron remains in the final state where there is also a Coulomb blockade, with a crossover in ground state from the empty dot state $|0\rangle$ to the single electron state $|e\rangle$ at a particular voltage. The significant point is that the X^0 - X^{1-} crossover occurs at a more negative voltage than the $|0\rangle - |e\rangle$ crossover. This is simply a consequence of the fact that the electron-hole Coulomb energy is larger than the electron-electron Coulomb energy, as revealed immediately in the red shift of the X^{1-} PL relative to the X^0 PL. This difference shifts the charging events with a hole to lower voltages than those without [7,8]. We account for this effect quantitatively by relating a change in applied gate voltage, ΔV_g , to the change in electrostatic potential, $e\Delta\phi$, with the lever arm λ (7 for this device), $\Delta\phi = \Delta V_g/\lambda$, and by assuming strong confinement, allowing the Coulomb interactions to be treated with Coulomb matrix elements. The model is fully defined with the electron-electron Coulomb energy, E_{ee} , the electron-hole Coulomb energy, E_{eh} , the quantum dot electron ionization energy, $E_{ionization}$, and the Schottky barrier at the surface, eV_s . We determine these parameters from the energy shift in the PL between the X^0 and X^{1-} excitons ($E_{eh} - E_{ee}$), the voltage extent of the X^0 plateau ($\lambda E_{ee}/e$), and the voltage of the X^0 - X^{1-} transition [$V_s - (\lambda/e)(E_{ionization} + E_{eh} - E_{ee})$]. Figure 3 is a plot of the energies versus V_g for the set of states without a hole, and with a hole for dot A. At the low bias end of the X^{1-} plateau, the final state after photon detection is $|e\rangle$, which lies above the $|0\rangle$ level. This means that the electron is unstable with respect to elastic tunneling into the continuum. The broad X^{1-} PL at the crossover voltage therefore reflects the fast tunneling, the linewidth Γ related to the tunneling time through $\Gamma = \hbar/\tau_t$. At more positive voltage, Fig. 2 shows that the $|e\rangle$ state becomes degenerate with the Fermi energy. This point is close to the inflexion point of the PL energy emphasizing the role of the continuum in determining the dot PL spectrum. At larger

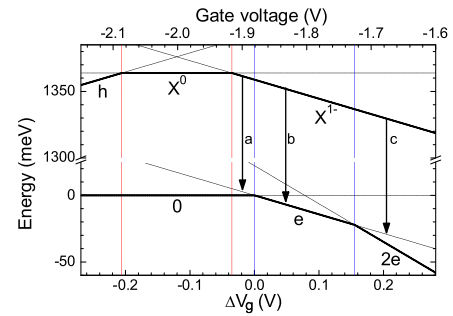


FIG. 3 (color online). Gate voltage dependence of the states h , X^0 , and X^{1-} all containing one hole; and states $|0\rangle$, $|e\rangle$, and $|2e\rangle$ without a hole. The PL transitions are from X^0 to $|0\rangle$ and from X^{1-} to $|e\rangle$. The parameters are chosen to model dot A. The bold lines follow the ground state energy in the two cases. Three regions of X^{1-} PL are labeled: a, where the final state is unstable with respect to elastic tunneling out of the dot; b, where the final state is stable with respect to elastic tunneling; and c, where the dot is unstable with respect to elastic tunneling into the dot.

V_g , the $|e\rangle$ state forms the final state ground state and elastic tunneling is forbidden, at which point the X^{1-} PL becomes symmetric with a small linewidth. Finally, at much larger V_g , the energies of the $|2e\rangle$ and $|e\rangle$ states cross such that the X^{1-} final state now becomes unstable with respect to tunneling of a continuum electron *into* the dot. The data show a broadening and anomalous dispersion exactly at the voltage predicted by this model (Fig. 1).

The correspondence between the anomalous features in Fig. 1 and the Coulomb blockade in Fig. 3 demonstrates that electron tunneling is at the heart of the anomalous PL. At the X^0 - X^{1-} crossover, the X^{1-} PL is broadened through rapid tunneling in the final state. The electron tunnels out and relaxes rapidly into the Fermi sea. However, close to the $|0\rangle - |e\rangle$ crossover in the final state, the PL takes on an asymmetric form. This points to a much more profound tunneling interaction with the continuum. We can prove this experimentally by raising the temperature. At 20 K (where the X^0 homogeneous broadening is still smaller than our experimental resolution), the anomalous X^{1-} PL loses its asymmetry, a consequence of the softening of the Fermi distribution in the Fermi sea. The asymmetric line shape therefore points to a partially coherent tunneling process, equivalently a final state which is a hybridization of dot and continuum states. To understand the quantum mechanics of this process, we calculate the optical emission by assuming that the system can be described by the Anderson Hamiltonian and that low energy excitations of the Fermi sea are unimportant (frozen Fermi sea).

The initial state is $|X^{1-}\rangle$ with energy E_i and is of pure quantum dot character; photon detection projects the system into the final state, $|f\rangle$ which is formed from $|e\rangle$ with energy E_e , describing an electron localized to the quantum dot, and the set $|k\rangle$ of continuum states with energy E_k : $|f\rangle = A_e|e\rangle + \sum_k A_k|k\rangle$. The exciton annihilation-photon creation operator is $V_{XP} = V_C^+ c_X$. There is a strong matrix element connecting $|e\rangle$ and $|X^{1-}\rangle$: $|\langle e|V_{XP}|X^{1-}\rangle|^2 = |V|^2$. However, the transition between the dot and the continuum transition is very weak and we take $\langle k|V_{XP}|X^{1-}\rangle \approx 0$ here. This can be expected on account of the very small overlap of the quantum dot and continuum wave functions. Experimentally, it can be justified from the very weak Fano effects recorded in laser spectroscopy on the X^{1-} on these structures [9], the Fano effect requiring for its observation a nonzero dot-continuum tran-

sition. The Anderson Hamiltonian operates on $|f\rangle$, $H_f|f\rangle = E_f|f\rangle$ with $H_f = E_e c_e^+ c_e + \sum_k E_k c_k^+ c_k + H_t$ where the first two terms denote the kinetic energy of the dot and continuum, respectively, and H_t describes elastic tunneling, $H_t = \sum_k (V_k c_k^+ c_e + V_k^* c_e^+ c_k)$. H_t couples the quantum dot and continuum states. The PL intensity is proportional to $I(\omega) = \sum_f |\langle f|V_{XP}|X^{1-}\rangle|^2 \delta(E_i - E_f - \hbar\omega)$. We replace the Dirac delta function with $\frac{1}{\pi} \Re\{\int_0^\infty \exp[i(E_i - E_f - \hbar\omega)t - \gamma t] dt\}$ thereby introducing a homogeneous broadening γ . The homogeneous broadening has been measured in laser spectroscopy [10] and contains a contribution from spontaneous emission ($\sim 1 \mu\text{eV}$) and at least one other dephasing process which broadens the lines to typically 2–5 μeV . This substitution gives $I(\omega) = \frac{|V|^2}{\pi} \Re\{\int_0^\infty \sum_f \langle e| \exp[i(E_i - H_f - \hbar\omega)t - \gamma t] |f\rangle \langle f|e\rangle dt\}$. Operator algebra then leads to $I(\omega) = \frac{|V|^2}{\pi} \Re\{\frac{i}{E_i - (E_e + E^*) - \hbar\omega + i\gamma}\}$ with the self-energy $E^* = \sum_k \frac{|V_k|^2}{E_i - E_k - \hbar\omega + i\gamma}$. This is an exact result; we now introduce some simplifications to give a reliable estimate of the self-energy. First, we model the electron reservoir as a two-dimensional electron gas (2DEG) with constant density of states, g , with a large bandwidth E_1 of occupied states. Second, E_i depends on V_g which we include with the lever arm approximation. Defining the Fermi energy to lie at zero energy, replacing V_g by ΔV_g , the voltage measured from the $|0\rangle - |e\rangle$ crossover point in Fig. 2, and measuring $\hbar\omega$ with respect to the unperturbed PL response, we find that the $E_i = -\frac{e}{\lambda} \Delta V_g$. Third, $|V_k|^2$ must decrease with increasing k through momentum conservation: the dot can only provide k up to $\sim 1/l_e$ where l_e is the lateral extent of wave function $|e\rangle$. The details of the k -dependence of V_k are not crucial, and it would be very involved to calculate them fully; we take $|V_k|^2$ to be a constant, V_0^2 , up to energy E_2 and zero thereafter. The conservation of momentum argument implies $E_1 + E_2 \approx \hbar^2/2m^*m_0l_e^2$. Fourth, we include occupation of the Fermi sea through the Fermi factor, $f_F(E) = [\exp(E/k_B T) + 1]^{-1}$, essentially treating the Fermi sea as a frozen spectator to the tunneling processes. We define the tunneling energy as $\Delta = 2\pi|V_0|^2 g$, related to the tunneling time τ_t by $\tau_t = \hbar/\Delta$. Finally, we include tunneling into the dot creating the $|2e\rangle$ final state with an additional contribution to the self-energy. Our final result for the optical response is

$$I(\omega) = \frac{I_0}{\pi} \Re\left\{ \frac{i}{-\hbar\omega + i\gamma - \frac{\Delta}{2\pi} \int_{-E_1}^{E_2} dE \left[\frac{1-f_F(E)}{-\frac{e}{\lambda}\Delta V_g - E - \hbar\omega + i\gamma} + \frac{f_F(E)}{\frac{e}{\lambda}\Delta V_g - E_{cc} + E - \hbar\omega + i\gamma} \right]} \right\}.$$

Example results of the theory are shown in Fig. 4 as a function of ΔV_g . At $\Delta V_g \sim -35$ mV, the peak of the spectrum lies close to the unperturbed value (zero in Fig. 4) with energy width Δ as a result of fast electron tunneling. At $\Delta V_g \sim 75$ mV, electron tunneling does not broaden the PL, but surprisingly it does lead to a noticeable

energy shift. In between these two regimes, the calculated spectrum shows first a strong blueshift followed by a strong redshift with increasing ΔV_g . For $\Delta V_g \sim 0$, the calculated PL is asymmetric with a tail extending to low energy. In all these respects, the theory mimics the experimental data. To make a quantitative comparison, we determine Δ from the

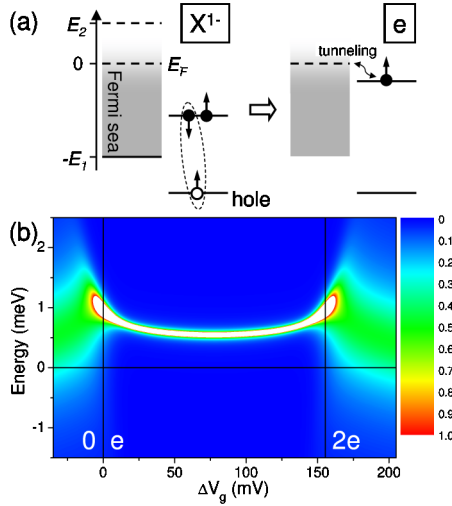


FIG. 4 (color online). (a) Schematic level diagram of the X^{1-} recombination process. (b) Calculated PL intensity versus gate voltage for a dot with tunnel energy $\Delta = 1.35$ meV, $T = 6$ K, and $I_0 = 1$, with the other parameters as in Fig. 2 but without a convolution of the spectrometer response.

PL at large and negative ΔV_g ; we take $\gamma = 5 \mu\text{eV}$ [10]; we use the Coulomb blockade model to deduce E_{ee} , the PL energy of an unperturbed X^{1-} and the V_g corresponding to $\Delta V_g = 0$; we take $E_1 = 30$ meV corresponding to the Fermi energy of the back contact, approximating it as a 2DEG with density 10^{12} cm^{-2} ; $E_2 = 30$ meV based on $l_e \approx 3$ meV; we convolute the theoretical spectrum with the response of the spectrometer, a Lorentzian with full width $50 \mu\text{eV}$; we set $T = 6$ K to account for slight local heating in the experiment; and we determine I_0 from the data at $\Delta V_g = -25$ mV. Figure 2 shows that the theory reproduces the measured energy shifts and changes in line shape and intensity extremely well. In particular, the distorted line shape at $\Delta V_g = -5$ mV is reproduced almost perfectly. The energy shifts are reproduced well for negative ΔV_g ; for positive ΔV_g , there is a small discrepancy. This could be related to a more complicated energy dependence of the tunneling matrix element or to the Stark effect if the Stark effect makes a positive contribution to the electron energy with increasing ΔV_g in this region, the Stark effect having a magnified effect on the response through electron tunneling. Unfortunately, we have no simple way of resolving the electron and hole Stark effects individually to include the Stark effect in the theory.

The significant point that emerges is that tunneling admixes a band of continuum states to the quantum dot state, not just the particular k state degenerate with the dot state, Fig. 4(a). The amount of admixture decreases as the energy difference increases. This is reminiscent of Kondo physics. A simple interpretation is that the electron can tunnel from the dot state $|e\rangle$ to a continuum state $|k\rangle$ changing its energy by δE on the time scale $\sim \hbar/\delta E$. If $\hbar/\delta E$ is less than or comparable to the tunneling time, then

this state can be accessed and is an important part of the final state. These effects are included in our calculation of the self-energy. We note that this effect is not an example of a Fano resonance as, first, it arises in emission rather than absorption, and second, as mentioned above, a Fano resonance would require a nonzero dot-continuum dipole matrix element. In principle, our scheme could project the system into a highly-correlated Kondo state [11,12]. This will likely be revealed with a stronger tunneling interaction, which could be achieved by narrowing the tunneling barrier in the device, a lower temperature, and a higher-mobility Fermi sea.

In conclusion, we present a spectroscopic signature of a hybridization between a localized quantum state and a Fermi sea. The effect manifests itself in the PL of a single quantum dot in a vertical electric field. The hybridization leads to an anomalous blueshift in the peak energy as well as a non-Lorentzian line shape.

We acknowledge financial support of this work from EPSRC (UK), DAAD, Alexander von Humboldt Stiftung and No. SFB 631 (Germany), and SANDiE (EU).

- [1] D. Goldhaber-Gordon, H. Shtrikman, D. Mahalu, D. Abusch-Magder, U. Meirav, and M. A. Kastner, *Nature (London)* **391**, 156 (1998).
- [2] J. Nygrd, D.H. Cobden, and P.E. Lindelof, *Nature (London)* **408**, 342 (2000).
- [3] J. Park, A.N. Pasupathy, J.I. Goldsmith, C. Chang, Y. Yaish, J.R. Petta, M. Rinkoski, J.P. Sethna, H.D. Abruña, P.L. McEuen, and D.C. Ralph, *Nature (London)* **417**, 722 (2002); W. Liang, M.P. Shores, M. Bockrath, J.R. Long, and H. Park, *Nature (London)* **417**, 725 (2002).
- [4] U. Fano, *Phys. Rev.* **124**, 1866 (1961).
- [5] R. J. Warburton, C. Schäflein, D. Haft, F. Bickel, A. Lorke, K. Karrai, J. M. Garcia, W. Schoenfeld, and P. M. Petroff, *Nature (London)* **405**, 926 (2000).
- [6] J. M. Smith, P. A. Dalgarno, R. J. Warburton, K. Karrai, B. D. Gerardot, and P. M. Petroff, *Phys. Rev. Lett.* **94**, 197402 (2005).
- [7] S. Seidl, M. Kroner, P. A. Dalgarno, J. M. Smith, A. Högele, M. Ediger, B. D. Gerardot, J. M. Garcia, P. M. Petroff, K. Karrai, and R. J. Warburton, *Phys. Rev. B* **72**, 195339 (2005).
- [8] S. Laurent, B. Eble, O. Krebs, A. Lemaître, B. Urbaszek, X. Marie, T. Amand, and P. Voisin, *Phys. Rev. Lett.* **94**, 147401 (2005).
- [9] M. Kroner, A. O. Govorov, S. Remi, B. Biedermann, S. Seidl, A. Badolato, P. M. Petroff, W. Zhang, R. Barbour, B. D. Gerardot, R. J. Warburton, and K. Karrai, *Nature (London)* **451**, 311 (2008).
- [10] A. Högele, S. Seidl, M. Kroner, K. Karrai, R. J. Warburton, B. D. Gerardot, and P. M. Petroff, *Phys. Rev. Lett.* **93**, 217401 (2004).
- [11] A. O. Govorov, K. Karrai, and R. J. Warburton, *Phys. Rev. B* **67**, 241307 (2003).
- [12] R. W. Helmes, M. Sindel, L. Borda, and J. von Delft, *Phys. Rev. B* **72**, 125301 (2005).